International Psychogeriatrics (2017), 29:5, 805–814 © International Psychogeriatric Association 2017
doi:10.1017/S1041610216002477

Aberrant interhemispheric functional connectivity within default mode network and its relationships with neurocognitive features in cognitively normal APOE ε 4 elderly carriers

Hanna Lu,[1,2] Suk Ling Ma,[1] Savio Wai Ho Wong,[3] Cindy W. C. Tam,[1] Sheung-Tak Cheng,[4] Sandra S. M. Chan[1] and Linda C. W. Lam[1]

[1]*Department of Psychiatry, The Chinese University of Hong Kong, G/F Multicenter, Tai Po Hospital, Hong Kong SAR, China*
[2]*Department of Psychiatry, Guangzhou Brain Hospital, The Affiliated Hospital of Guangzhou Medical University, Guangzhou, China*
[3]*Department of Special Education and Counselling, Hong Kong Institute of Education Center for Brain and Education, The Hong Kong Institute of Education, Hong Kong SAR, China*
[4]*Department of Health and Physical Education, The Education University of Hong Kong, Hong Kong SAR, China*

ABSTRACT

Background: Default mode network (DMN) is vulnerable to the effects of APOE genotype. Given the reduced brain volumes and APOE ε 4-related brain changes in elderly carriers, it is less known that whether these changes would influence the functional connectivity and to what extent. This study aimed to examine the functional connectivity within DMN, and its diagnostic value with age-related morphometric alterations considered.

Methods: Whole brain and seed-based resting-state functional connectivity (RSFC) analysis were conducted in cognitively normal APOE ε 4 carriers and matched non-carriers ($N = 38$). The absolute values of mean correlation coefficients (z-values) were used as a measure of functional connectivity strength (FCS) between DMN subregions, which were also used to estimate their diagnostic value by receiver-operating characteristic (ROC) curves.

Results: APOE ε 4 carriers demonstrated decreased interhemispheric FCS, particularly between right hippocampal formation (R.HF) and left inferior parietal lobular (L.IPL) ($t = 3.487$, $p < 0.001$). ROC analysis showed that the FCS of R.HF and L.IPL could differentiate APOE ε 4 carriers from healthy counterparts (AUC value = 0.734, $p = 0.025$). Moreover, after adjusting the impact of morphometry, the differentiated value of FCS of R.HF and L.IPL was markedly improved (AUC value = 0.828, $p = 0.002$).

Conclusions: Our findings suggest that APOE ε 4 allele affects the functional connectivity within posterior DMN, particularly the atrophy-corrected interhemispheric FCS before the clinical expression of neurodegenerative disease.

Key words: apolipoprotein E, functional connectivity, default mode network, neurocognitive disorder, Alzheimer's disease

Introduction

Dementia, including Alzheimer's disease (AD), is one of the most therapeutically intractable global healthy challenges and may affect up to 135 million adults worldwide by 2050 (Prince *et al.*, 2013). There is an emerging need to examine and identify the disease-specific biomarkers characterized by genetic and neuroimaging investigations to differentiate the individuals with high risks of developing neurodegenerative disease. Apolipoprotein E (APOE) ε 4 allele, as one of the well-replicated genetic risk factor for sporadic AD (Corder, *et al.*, 1993; Saunders *et al.*, 1993; Liu *et al.*, 2013), attends the formulation of β-amyloid (Aβ) (Mahley *et al.*, 2006). Compelling evidence has demonstrated that the Aβ, as a pathological hallmark of AD, deposits and spreads progressively in some brain regions from the starting point

Correspondence should be addressed to: Dr Hanna Lu and Prof Linda C. W. Lam, Address: Department of Psychiatry, The Chinese University of Hong Kong, G/F Multicenter, Tai Po Hospital, Tai Po, Hong Kong, SAR China. Phone: +(852) 2831–4305; Fax: +(852) 2667–5464. Email: hannalu@cuhk.edu.hk; cwlam@cuhk.edu.hk. Received 1 Sep 2016; revision requested 10 Oct 2016; revised version received 15 Dec 2016; accepted 20 Dec 2016. First published online 26 January 2017.

of AD pathophysiological cascade (Braak *et al.*, 1991; Buckner *et al.*, 2005; Bero *et al.*, 2011; Jack *et al.*, 2013). Of particular interest, the functional organizations of these brain regions are embedded in a critical brain circuit, which is called "default mode network" (DMN) (Fox *et al.*, 2005; Sperling *et al.*, 2009).

DMN refers to a collection of brain regions that demonstrate reduced activity during attention-demanding tasks and increased activity during the state of "task-free" (Buckner and Vincent, 2007). Toward a "two-level" feature of the DMN (Lu *et al.*, 2016), each subregion of DMN coordinate with each other to participate in various cognitive function; meanwhile, these areas also play critical roles in various cognition-specific processes. For instance, medial prefrontal cortex (mPFC) was involved in decision making (Szczepanski and Knight, 2014), lateral temporal cortex (LTC), and hippocampal formation (HF) was involved in retrieving memory (Wikenheiser and Redish, 2012), inferior parietal lobe (IPL) was involved in attention shifting (Peterson and Posner, 2012), posterior cingulate gyrus (PCG) was involved in cognitive control (Leech and Sharp, 2014).

Evidence from resting-state functional magnetic resonance imaging (rs-fMRI) has confirmed the aberrant functional connectivity (FC) within DMN in APOE ε 4 carriers with middle age (Goveas *et al.*, 2013; Wu *et al.*, 2016) and old age (Vemuri *et al.*, 2010). Beyond the qualitative evaluation, some burgeoning researches have attempted to examine the effects of APOE ε 4 on functional connectivity strength (FCS) between DMN subregions. Early evidence from task-related fMRI found that APOE ε 4 young carriers showed an increased coactivation of DMN subregions during an encoding memory task, particularly in right hippocampus (Filippini *et al.*, 2009). Later, several decreased connectivity within posterior DMN (pDMN), including PCG, precuneus, and left IPL, was found in APOE ε 4 AD patients (Jones *et al.*, 2011). Recently, this modulating effect of APOE ε 4 has been found on the decreased intramodular connectivity within pDMN in AD patients (Wang *et al.*, 2015).

It is valuable to notice the nascent evidence that the disturbance of FC within DMN is not just restricted to the impacts of pathological factors (i.e. APOE ε 4), but also associated with the coupled changes under the aging process (Davies *et al.*, 2014). Of note, given the APOE ε 4-related cortical changes reported in our recent work (Lu *et al.*, 2016), whether the APOE ε 4 elderly carriers display a different pattern of FC within DMN with or without atrophy adjusted awaits further investigation. Regard to this, we aimed to investigate the atrophy-corrected FCS within DMN. To achieve this aim, a two-step strategy based on two analytical methods was launched: (1) we conducted the whole-brain and seed-based FC by resting-state fMRI analysis with or without morphometric differences adjusted; (2) we tested whether the differences of FCS within DMN could differentiate the APOE ε 4 carriers from non-carriers.

Materials and methods

Participants

Thirty-eight community-dwelling right-handed adults (aged between 65 and 80 years) who were the participants in our previous study (Lu *et al.*, 2016) were included in this work. A neuropsychological battery, APOE genotyping, and rs-fMRI were conducted. Written informed consent from all participants was obtained before the cognitive evaluation and APOE genotyping. Ethics approval was obtained from the Joint Chinese University of Hong Kong-New territories East Cluster Clinical Research Ethics Committee (Joint CUHK-NTECCREC).

Apolipoprotein E genotyping

All participants provided a sample of DNA for APOE genotyping. Genomic DNA was extracted from peripheral blood samples using DNA extraction kit according to the instruction (Qiagen, US). The presence of APOE ε 2, APOE ε 3, and APOE ε 4 alleles were analyzed and performed using PCR-RFLP, which was well validated and described in our previous work (Ma *et al.*, 2005).

Neurocognitive assessment and clinical evaluation

A standardized neuropsychological battery was employed to evaluate the global cognition and major domains of cognition, which has been described previously (Lu *et al.*, 2016). Cantonese Mini-Mental State Examination (CMMSE) and Alzheimer's Disease Assessment Scale cognitive subscale (ADAS-Cog) were used as a measure of global cognition. Delayed recall of words and digit span backward (DSB) were used to evaluate the episodic memory. Digit span forward (DSF) and trail making test part A (TMT-A) were used to assess the functioning of attention. Chinese verbal fluency test (CVFT) and trail making test part B (TMT-B) were used to assess the performance of executive function. All the measurements were conducted with Chinese instructions.

Resting-state functional MRI (rs-fMRI)

All MRI images were acquired in the Prince of Walsh Hospital (Hong Kong) by using a

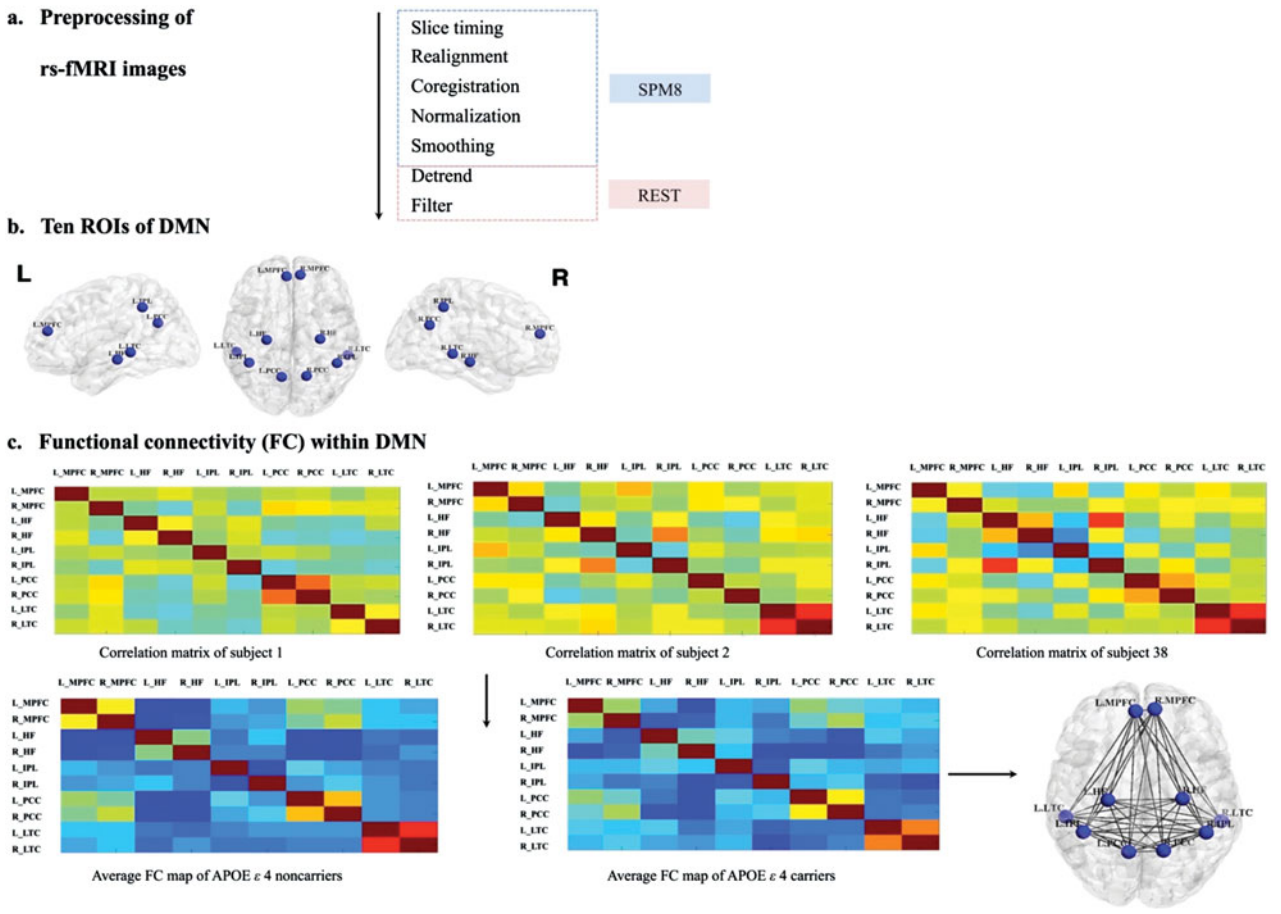

Figure 1. (Colour online) The flowchart of rs-fMRI analysis. After preprocessing (1), the functional connectivity strength (FCS) within DMN was calculated between each ROI (2) individually (3) by means of Fisher's *z* transformed Pearson correlation coefficient (*z*-value). (4) The visualization of ROIs and connections were performed by Brain Net Viewer (Xia *et al.*, 2013).

3T Philips MRI scanner (Achieva TX, Philips Medical System, Best, the Netherlands) with an eight-channel SENSE head coil. A series of 3D high-resolution T1-weighted anatomical images were obtained for each elderly with the following parameters (Lu *et al.*, 2016): repetition time (TR) = 7.4 ms, echo time (TE) = 3.4 ms, flip angle = 8°, voxel size = 1.04 × 1.04 × 0.6 mm^3.

During the session of resting-state fMRI, all participants were instructed to relax and keep their eyes close. To ensure the quality of rs-fMRI data, participants were immediately addressed after each rs-fMRI run via the intercom to ensure they stay awake in the scanner. In each scanning sequence, we obtained a series of 40 axial T2-weighted gradient echo-planar images (TR = 3000 ms, TE = 25 ms, flip angle = 90°, field of view (FOV) = 230 × 230 mm^2, in-plane resolution = 2.4 × 2.4 mm^2, matrix = 96 × 96, slice thickness = 3 mm). A total of 120 time points of rs-fMRI were acquired for each participant (Lou *et al.*, 2015).

Resting state fMRI preprocessing and analysis

Preprocessing of rs-fMRI images was conducted by Statistical Parametric Mapping software (SPM8, http://www.fil.ion.ucl.ac.uk/spm/software/spm8/) and resting-state fMRI data analysis toolkit (REST, http://restfmri.net/forum/REST_V1.8) (Song *et al.*, 2011) embedded in MATLAB R2012b. The first five volumes of each functional time series were discarded because of the instability of the initial MRI signal and initial adaption of participants to the situation. As depicted in Figure 1a, the remaining rs-MRI data was subsequently corrected for slice timing and realigned to the first image by rigid-body head movement correction. Then, the rs-fMRI images were coregister to high-resolution T1 images and normalized to standard stereotaxic anatomical Montreal Neurological Institute (MNI) space. The normalized volumes were spatially smoothed using an isotropic Gaussian filter of 8-mm full width at half maximum.

The time series in each voxel was detrended to correct for linear drift over time. Nuisance signal

Table 1. Five pairs of ROIs within default mode network

BRAIN REGIONS	ABBREVIATIONS	AAL LABELS	BRODMANN AREA
Medial prefrontal cortex	MPFC	Frontal_sup_medial_L/R	BA 10
Posterior cingulate cortex	PCC	Cingulate_post_L/R	BA 30
		Precuneus_L/R	BA 23
Inferior parietal lobule	IPL	Partietal_inf_L/R	BA39, BA 40
Hippocampal formation	HF	Hippocampus_L/R	BA 27, 28, 34, 35, 36
Lateral temporal cortex	LTC	Temporal_inf_L/R	BA21

Note. AAL = Automated Anatomical Labeling.

(whole brain, white matter, cerebrospinal fluid, and six motion parameters) were regressed out from the rs-fMRI time series (Vergun *et al.*, 2013; Manza *et al.*, 2015). Subsequently, temporal filtering with a band of 0.01–0.08 Hz was conducted to the time series of each voxel to reduce the impact of low-frequency drifts and high-frequency noise (Ding *et al.*, 2013). Then, the above preprocessed rs-fMRI images were used for FC analysis.

Functional connectivity analysis

First, given the well-defined functional anatomy of default network (Fox *et al.*, 2005; Buckner *et al.*, 2008), five pairs of brain areas are selected as regions of interest (ROIs) (Figure 1b): IPL, medial prefrontal gyrus (mPFC), HF, posterior cingulate cortex (PCC), and LTC. The masks of ROIs were generated by the WFU Pick Atlas (http://fmri.wfubmc.edu/software/PickAtlas) corresponding to the anatomical regions embedded in the Automated Anatomical Labeling (AAL) (Table 1).

Second, the mean time courses were extracted from each ROI by averaging the time courses over all voxels within the ROI. To better illustrate the functional organization of DMN subregions, whole-brain and ROI-wise FC were employed. For whole-brain FC, Pearson correlation coefficients were calculated between each ROI and the whole brain areas embedded in the AAL atlas (Salvador *et al.*, 2005). After Fisher's z transformation, individual FC map was used for group-wise comparison. For ROI-wise FC, Pearson correlation coefficients were calculated between the corrected time series of the ROIs. The absolute value of correlation coefficient (r) was used as a measure to evaluate the FCS between the ROIs (Diwadkar *et al.*, 2000; Dai *et al.*, 2014; Li *et al.*, 2014). Smaller value of FCS indicates the decreased connectivity between DMN subregions.

Statistical analyses

Group-wise differences of demographics and scores of neurocognitive tasks were tested either with χ^2 for categorical variable or independent two sample t-test for continuous variables. Comparisons of whole-brain and ROI-wise FC maps were conducted by two-sample t-test embedded in REST. As to the whole-brain FC, family wise error (FWE) correction with p value of 0.05 was addressed. As to the ROI-wise FC, the correlation matrix of ten DMN subregions was performed individually (Figure 1c). Bonferroni correction (Jiang *et al.*, 2004; Watanabe *et al.*, 2013) was used to reduce the chances of obtaining false-positive results. Given the ten predefined ROIs, we would have $10 \times (10-1)/2 = 45$ pairwise comparisons, the adjusted p value would be $0.05/45 = 0.00111$. Finally, the receiving operating characteristic (ROC) curves were used to evaluate whether the FCS within DMN could discriminate APOE ε 4 carriers from non-carriers. The χ^2 test, two sample t-test, Pearson correlation coefficients, and ROC analysis were performed by IBM SPSS Statistics (Version 20).

Results

Demographics and neurocognitive features

As Table 2 shown, the demographics in term of age, gender, years of education were similar between APOE ε 4 carriers and healthy controls. The global cognition and the functioning cross the cognitive domains between two groups were also comparable. While, there was a trend that APOE ε 4 carriers presented worse performance on global cognition (ADAS-Cog) and episodic memory (DSB and delayed recall of words) and better performance on attention (TMT-A) and executive function (TMT-B and CVFT) than non-carriers.

Comparison of functional connectivity

With age, gender, and years of education as covariates, no significant difference was found in whole-brain FC maps between two groups with a threshold of FWE corrected $p < 0.05$.

Table 2. Demographics and neurocognitive characteristics

	APOE ε 4 CARRIERS (N= 11)	APOE ε 4 NON-CARRIERS (N= 27)	T VALUE (χ^2)	p VALUE
Age	69.48 ± 4.41	70.40 ± 4.35	0.584	0.913
Gender (F/M)	7/4	17/10	− 0.038	0.97
Education (years)	7.00 ± 4.27	8.48 ± 3.88	1.038	0.306
CMMSE	27.36 ± 3.01	27.81 ± 2.39	0.49	0.627
ADAS-Cog	7.36 ± 2.25	6.19 ± 2.86	− 1.22	0.23
Delayed recall of words	6.09 ± 1.3	6.67 ± 1.52	1.101	0.278
Digit span backward	3.63 ± 1.29	4.07 ± 1.84	0.719	0.477
Chinese verbal fluency test	41.36 ± 10.54	39.89 ± 6.41	− 0.53	0.599
Trail making test B (second)	17.27 ± 10.64	20.56 ± 14.01	0.698	0.49
Digit span forward	7.09 ± 1.64	7.7 ± 1.23	1.260	0.216
Trail making test A (second)	13.27 ± 7.88	15.7 ± 10.45	0.381	0.706

Note. Data are raw scores and presented as mean ± standard deviation (SD).
CMMSE = Cantonese mini mental state examination; ADAS-Cog = Alzheimer's Disease Assessment Scale cognitive subscale.

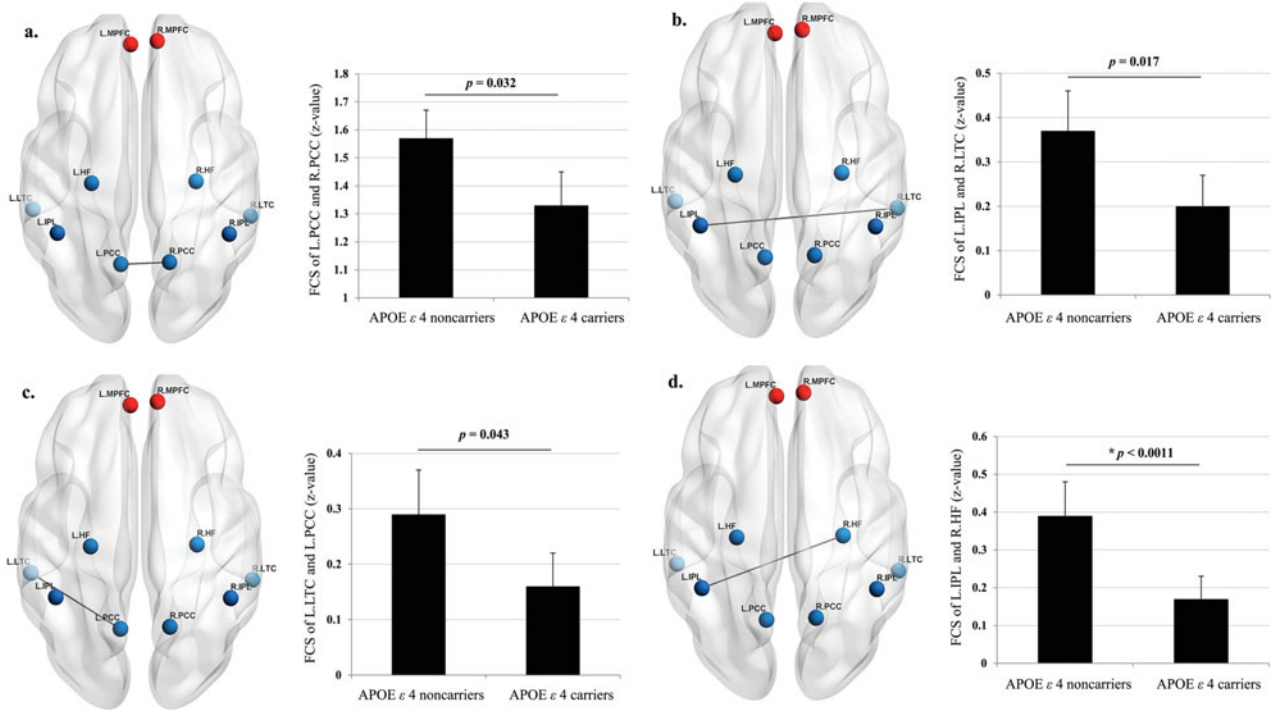

Figure 2. (Colour online) Group-wise differences of FCS within DMN. Four pairwise of FCS (a–d) are prominently decreased in APOE ε 4 elderly carriers with significant level of $p < 0.05$. Only the FCS of left inferior parietal lobe and right hippocampal formation (d) survived after Bonferroni correction.

Meanwhile, among 45 pairwise seed-based FC maps, prominent differences were found in the FCS of left PCC and right PCC ($t = 2.224$, $p = 0.032$, Figure 2a), left IPL and right LTC ($t = 2.509$, $p = 0.017$, Figure 2b), left PCC and left LTC ($t = 2.112$, $p = 0.043$, Figure 2c), right HF and left IPL ($t = 3.487$, $p = 0.001$) at the significant level of 0.05 (Table 3).

However, only the FCS of right HF and left IPL survived (Figure 2d) after Bonferroni correction (with an adjusted p value of 0.0011). These results indicate that APOE ε 4 elderly carriers display the relatively weaker FC within DMN than non-carriers, particularly the interhemispheric connectivity of pDMN.

Associations between age, neurocognitive function, and FCS

As shown in supplementary table (available as supplementary material attached to the electronic version of this paper at www.journals.cambridge.org/jid_IPG), chronological age was negatively associated with the FCS within DMN, such as

Table 3. Comparison of functional connectivity strength within DMN

FCS within DMN	APOE ε 4 carriers ($N = 11$)	APOE ε 4 non-carriers ($N = 27$)	T value	p value	95% CI	
					Lower	Upper
R.HF_L.IPL	0.17 ± 0.11	0.39 ± 0.28	3.487	**0.001***	0.092	0.349
L.IPL_R.LTC	0.20 ± 0.13	0.37 ± 0.29	2.509	0.017	0.033	0.311
L.PCC_R.PCC	1.33 ± 0.38	1.57 ± 0.25	2.224	0.032	0.021	0.447
L.PCC_L.LTC	0.16 ± 0.14	0.29 ± 0.23	2.112	0.043	0.004	0.261

Note. Data are raw scores and presented as mean ±SD.
*Significant after Bonferroni correction.

the FCS between right mPFC and left IPL ($r = -0.341$, $p = 0.039$) and the FCS of right mPFC and left LTC ($r = -0.376$, $p = 0.022$). The results suggest that the reduced FCS within DMN is coupling with advancing age. In addition, with age, gender, and years of education as covariates, FCS within DMN was prominently associated with the scores of neurocognitive performance, such as global cognition (CMMSE) was positively associated with the FCS of left PCC and right LTC ($r = 0.435$, $p = 0.009$) and the FSC of left HF and left IPL ($r = 0.428$, $p = 0.009$), and executive function was positively correlated with the FCS of left mPFC and right LTC (CVFT: $r = 0.431$, $p = 0.009$).

ROC curves

The analysis of ROC curves found none of the neurocognitive features presented a significant value to discriminate APOE ε 4 carriers from healthy controls. Instead, the interhemispheric FCS showed a moderate value, that was the area under the curve (AUC) of FCS of right HF and left IPL (AUC value = 0.734, $p = 0.025$, 95% CI [0.578, 0.890]) was prominently higher than the other FCS within DMN (Figure 3a), such as FCS of left IPL and right LTC (AUC value = 0.687, $p = 0.074$, 95% CI [0.519, 0.854]), FCS of left PCC and left LTC (AUC value = 0.667, $p = 0.111$, 95% CI [0.485, 0.849]), FCS of left PCC and right PCC (AUC value = 0.694, $p = 0.064$, 95% CI [0.493, 0.894]).

Given the group-wise difference of gray matter volume (GMV) reported in our recent work (Lu *et al.*, 2016), to further tackle the impacts of morphometric difference on the discriminative values of FCS, the GMV of right cingulate gyrus was used as a covariate. Of note, as Figure 3b depicted, the differentiated values of FCS within DMN were markedly improved, including right HF and left IPL: AUC value = 0.828, $p = 0.002$, 95% CI [0.689, 0.967]; left IPL and right LTC: AUC value = 0.761, $p = 0.013$, 95% CI [0.589, 0.933]; left PCC and right PCC: AUC value = 0.761, $p = 0.013$, 95% CI [0.585, 0.937]; left PCC and left LTC: AUC value = 0.754, $p = 0.015$, 95% CI [0.598, 0.911].

Discussion

In current study, we identified the resting-state FC within DMN using a measure of FCS and examined its associations with neurocognitive features in senior adults with genetic risk for neurodegeneration. Generally, APOE ε 4 elderly carriers, even though presented relatively normal cognition and non-significant brain atrophy, rather demonstrated the aberrant functional organizations within DMN. It is intriguing to find that the APOE ε 4 carriers showed the prominent weaker atrophy-corrected FCS of interhemispheric connectivity within DMN, which was also presented a utility to differentiate APOE ε 4 carriers from non-carriers.

Disrupted functional connectivity within DMN

Identifying the characteristics of functional organizations of shrinked cortex and their correlates with neurocognitive features is challenging. One of the reasons is that APOE ε 4 demonstrates differential effects on the individuals with different age range. For instance, APOE ε 4-related effects were more pronounced in older adults than the younger ones (Papenberg *et al.*, 2015). Besides, prior fMRI study also found the stronger effects of APOE ε 4 in senior adults with the presence of deceased activation in multiple brain regions, particularly in HF (Filippini *et al.*, 2011). Another reason is because of the age-related cognitive decline (ARCD) and its underlying morphometric change. Mounting and robust relationships between disturbed FC within DMN, advancing age, and worse neurocognitive function implicates the potential impacts from the age-morphometry coupling changes.

Consistent with previous evidence (Luo *et al.*, 2016), reduced interhemispheric FC within DMN

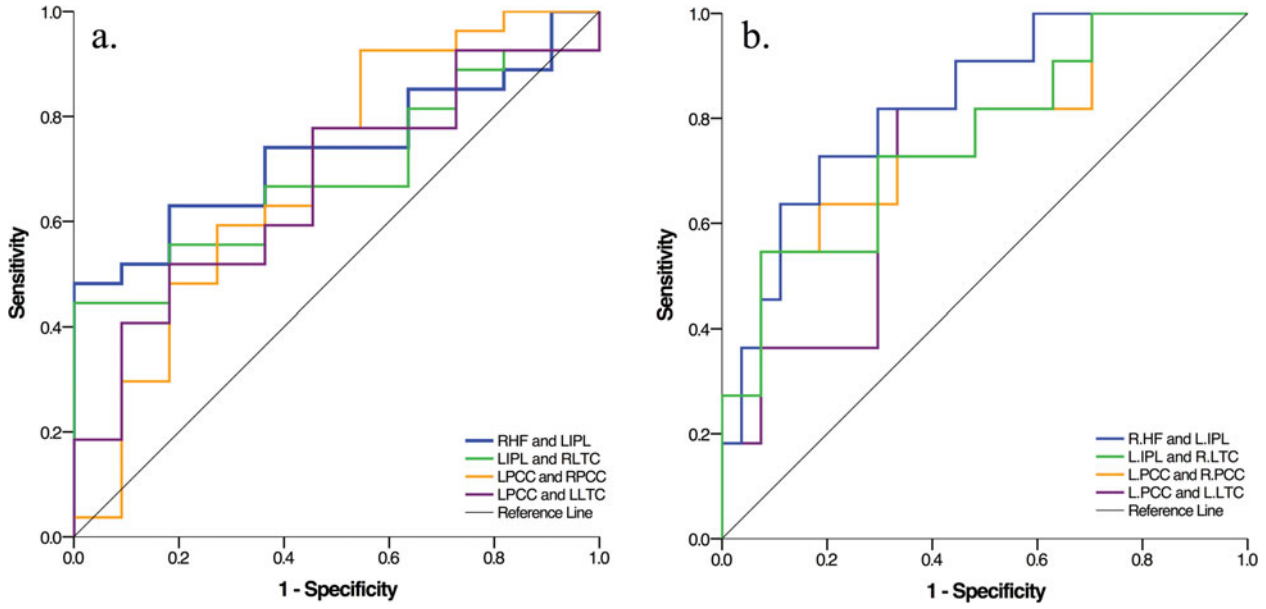

Figure 3. (Colour online) Receiver operator characteristic (ROC) curves for the FCS within DMN. The FCS of right hippocampal formation and left inferior parietal lobe presents a modest power to differentiate APOE ε 4 carriers from healthy controls (3a). While, the differentiated values of the FCS within DMN were markedly improved after adjusting the morphometric atrophy (3b).

were found in APOE ε 4 elderly carriers. The interhemispheric aberrance highlights a possibility that the prodromal impacts of APOE ε 4 may present with the dysfunction of coordination and integration between the two brain hemispheres. Even though the mechanisms that contribute to the difference of FCS in APOE ε 4 elderly carriers remain a cornerstone, the possible explanations could be postulated from two aspects. On one side, the pattern of Aβ deposition in cortex is aligned with the trajectory of disease progression described in Braak's hypothesis (Braak and Braak, 1991; De Leon *et al.*, 2001), especially the regions involved in DMN (Sperling *et al.*, 2009). On the other side, the heterogeneity of DMN subregions affiliated with cognition-specific sub-networks is also expended to the different connectivity patterns. For instance, anterior DMN (aDMN) includes anterior cingulate cortex (ACC) and mPFC; pDMN contains PCC, IPL, HF, and LTC. Of note, HF atrophy has been regarded as a robust marker to predict the conversion from mild cognitive impairment (MCI) to AD (Sluimer *et al.*, 2008; Tondelli *et al.*, 2012), which also highlights the functional modularity of HF implemented by pDMN.

Interhemispheric FC as a promising indicator

With the advances in resting state FC MRI, AD has been reframed as a syndrome of "disconnectivity" with the presence of disturbed functional or structural connectivity (Delbeuck *et al.*, 2003). Converging evidence from fMRI studies shows that the disturbance of FC within DMN is common in the individuals with subtypes of MCI and AD (Greicius *et al.*, 2004; Sheline and Raichle, 2013). Notably, the aberrant changes of FC embedded in pDMN have presented great variations than aDMN from an individual level (Kim and Lee, 2011), which suggest pDMN maybe more vulnerable to the pathological factors (Jones *et al.*, 2011; Damoiseau *et al.*, 2012). Based on our observations, it is not surprising to identify the marked age-related deceased of FCS within DMN in elderly carriers. Beyond group-wise differences, our results also supported that APOE ε 4 allele may have a selective impact on the interhemispheric FC within pDMN, even in the context of relatively normal cognition. Of particular interest, the FCS of right HF and left IPL not just demonstrated a utility to differentiate the APOE ε 4 carriers from healthy controls, but also showed an improved differentiated value when accounting for the effects of morphometric difference.

Related to the functional connections, the early changes of interhemispheric FC have been found within pDMN (Machulda *et al.*, 2011; Donix *et al.*, 2013; Luo *et al.*, 2016). What our results extend the prior evidence is that the interhemispheric FC within pDMN might be an impending indicator to distinguish healthy elderly from the individuals with genetic risk for AD. Additionally, the enhanced differentiated values of atrophy-corrected FCS within DMN also highlights a better understanding of the structural–functional coupling changes in APOE ε 4 elderly carriers.

Limitations and future works

The findings of the present study should be circumspectly interpreted with its limitations. First, the cross-sectional design with a small sample size might limit the generalizability of the results. Second, the backgrounds of physical activity, fitness, and cerebrovascular risk factors are not included in this study, which might affect the strength of FC as well. Third, we only focused on the genetic risk of APOE ε 4 allele and default network; the potential effects of APOE ε 2 and other intrinsic connectivity network were not launched. Fourth, all participants were from Chinese community, which may not give an accurate reflection of the characteristics of senior adults with various cultural backgrounds.

Further work is required to validate our findings in a longitudinal cohort with a relatively large sample size. Combined with the morphometric features, it will be intriguing to examine the potential effects of APOE ε 4 on structural and functional lateralization. Besides, the reduced FC within DMN would be employed as "connectivity of interest" to examine the structural–functional correlates using diffusion tensor imaging (DTI).

Conflict of interest

None.

Description of authors' roles

Cindy W. C. Tam, Sheung-Tak Cheng, and Linda C. W. Lam conceived and designed this study. Suk Ling Ma conducted the APOE genotyping. Savio Wai Ho Wong performed the pre-processing of rs-fMRI images. Hanna Lu conducted the FC analysis and visualized the FC. As to this paper, Hanna Lu drafted, Sandra S. M. Chan and Linda C. W. Lam discussed and agreed with the final version.

Acknowledgments

This research was supported by the General Research Fund (GRF) Hong Kong. The authors thank Prof. Yong He, Dr Mingrui Xia, Dr Xuhong Liao, and Zaixu Cui from the State Key Laboratory of Cognitive Neuroscience and Learning & IDG/McGovern Institute for Brain Research, Beijing Normal University, and Dr Zhengjia Dai from the Department of Psychology, Sun Yat-sen University for their valuable suggestion of functional connectivity analysis. The authors also thank all the participants who served as the research participants and the reviewers for their valuable comments to improve the quality of the paper.

Supplementary material

To view supplementary material for this article, please visit https://doi.org/10.1017/S1041610216002477

References

Bero, A. W. *et al.* (2011). Neuronal activity regulates the regional vulnerability to amyloid-β deposition. *Nature Neuroscience*, 14, 750–756.

Braak, H. and Braak, E. (1991). Neuropathological stageing of Alzheimer-related changes. *Acta Neuropathologica*, 82, 239–259.

Buckner, R. L., Andrews-Hanna, J. R. and Schacter, D. L. (2008). The brain's default network: anatomy, function, and relevance to disease. *Annals of the New York Academy of Sciences*, 1124, 1–38.

Buckner, R. L. *et al.* (2005). Molecular, structural, and functional characterization of Alzheimer's disease: evidence for a relationship between default activity, amyloid, and memory. *Journal of Neuroscience*, 25, 7709–7717.

Buckner, R. L. and Vincent, J. L. (2007). Unrest at rest: default activity and spontaneous network correlations. *NeuroImage*, 37, 1091–1096.

Corder, E. H., Saunders, A. M., Strittmatter, W. J., Schmechel, D. E. and Gaskell, P. C. (1993). Gene dose of apolipoprotein E type 4 allele and the risk of Alzheimer's disease in late onset families. *Science*, 261, 921–923.

Dai, Z. *et al.* (2014). Identifying and mapping connectivity patterns of brain network hubs in Alzheimer's disease. Cereb Cortex, bhu246.

Damoiseaux, J. S., Prater, K. E., Miller, B. L. and Greicius, M. D. (2012). Functional connectivity tracks clinical deterioration in Alzheimer's disease. *Neurobiology Aging*, 33, 828.e19–30.

Davies, G. *et al.* (2014). A genome-wide association study implicates the ApoE locus in nonpathological cognitive ageing. *Molecular Psychiatry*, 19, 76–87.

De Leon, M. J. *et al.* (2001). Prediction of cognitive decline in normal elderly subjects with 2-[18F] fluoro-2-deoxy-D-glucose/positron-emission tomography (FDG/PET). *Proceedings of National Academy of Sciences USA*, 98, 10966–10971.

Delbeuck, X., Linden, M. V. D. and Collette, F. (2003). Alzheimer's disease as a disconnection syndrome?. *Neuropsychology Review*, 13, 79–92.

Ding, W. N. *et al.* (2013). Altered default network resting-state functional connectivity in adolescents with Internet gaming addiction. *PloS One*, 8, e59902.

Diwadkar, V. A., Carpenter, P. A. and Just, M. A. (2000). Collaborative activity between parietal and dorso-lateral prefrontal cortex in dynamic spatial working memory revealed by fMRI. *NeuroImage*, 12, 85–99.

Donix, M. *et al.* (2013). ApoE associated hemispheric asymmetry of entorhinal cortical thickness in aging and Alzheimer's disease. *Psychiatry Research*, 214, 212–220.

Filippini, N. *et al.* (2011). Differential effects of the APOE genotype on brain function across the lifespan. *Neuroimage*, 54, 602–610.

Filippini, N. *et al.* (2009). Anatomically-distinct genetic associations of ApoE epsilon4 allele load with regional cortical atrophy in Alzheimer's disease. *NeuroImage*, 44, 724–728.

Fox, M. D., Snyder, A. Z., Vincent, J. L., Corbetta, M., Van Essen, D. C. and Raichle, M. E. (2005). The human brain is intrinsically organized into dynamic, anticorrelated functional networks. *Proceedings of the National Academy of Sciences USA*, 102, 9673–9678.

Goveas, J. S. *et al.* (2013). Functional network endophenotypes unravel the effects of apolipoprotein E epsilon 4 in middle-aged adults. *PloS one*, 8, e55902.

Greicius, M. D., Srivastava, G., Reiss, A. L. and Menon, V. (2004). Default-mode network activity distinguishes Alzheimer's disease from healthy aging: evidence from functional MRI. *Proceedings of National Academy of Sciences U S A*, 101, 4637–4642.

Jack, C. R. *et al.* (2013). Tracking pathophysiological processes in Alzheimer's disease: an updated hypothetical model of dynamic biomarkers. *Lancet Neurology*, 12, 207–216.

Jiang, T., He, Y., Zang, Y. and Weng, X. (2004). Modulation of functional connectivity during the resting state and the motor task. *Human Brain Mapping*, 22, 63–71.

Jones, D. T. *et al.* (2011). Age-related changes in the default mode network are more advanced in Alzheimer disease. *Neurology*, 77, 1524–1531.

Kim, D. Y. and Lee, J. H. (2011). Are posterior default-mode networks more robust than anterior default-mode networks? evidence from resting-state fMRI data analysis. *Neuroscience Letters*, 498, 57–62.

Leech, R. and Sharp, D. J. (2014). The role of the posterior cingulate cortex in cognition and disease. *Brain*, 137, 12–32.

Li, R. *et al.* (2014). Multimodal intervention in older adults improves resting-state functional connectivity between the medial prefrontal cortex and medial temporal lobe. *Front Aging Neurosci*, 6, 39.

Liu, C. C., Kanekiyo, T., Xu, H. and Bu, G. (2013). Apolipoprotein E and Alzheimer disease: risk, mechanisms and therapy. *Nature Reviews Neurology*, 9, 106–118.

Lou, W. *et al.* (2015). Decreased activity with increased background network efficiency in amnestic MCI during a visuospatial working memory task. *Human Brain Mapping*, 36, 3387–3403.

Lu, H., Fung, A. W., Chan, S. S. and Lam, L. C. (2016). Disturbance of attention network functions in Chinese healthy older adults: an intra-individual perspective. *International Psychogeriatrics*, 28, 291–301.

Lu, H., Ma, S. L., Chan, S. S. and Lam, L. C. (2016). The effects of apolipoprotein ε 4 on aging brain in cognitively normal Chinese elderly: a surface-based morphometry study. *International Psychogeriatrics*, 28, 1503–1511.

Luo, X. *et al.* (2016). Decreased inter-hemispheric functional connectivity in cognitively intact elderly APOE ε4 carriers: a preliminary study. *Journal of Alzheimers Disease*, 50, 1137–1148.

Ma, S. L., Tang, N. L., Lam, L. C. and Chiu, H. F. (2005). The association between promoter polymorphism of the interleukin-10 gene and Alzheimer's disease. *Neurobiology of Aging*, 26, 1005–1010.

Machulda, M. M. *et al.* (2011). Effect of APOE ε4 status on intrinsic network connectivity in cognitively normal elderly subjects. *Archives of Neurology*, 68, 1131–1136.

Mahley, R. W., Weisgraber, K. H. and Huang, Y. (2006). Apolipoprotein E4: a causative factor and therapeutic target in neuropathology, including Alzheimer's disease. *Proceedings of the National Academy of Sciences USA*, 103, 5644–5651.

Manza, P., Zhang, S., Hu, S., Chao, H. H., Leung, H. C. and Chiang-shan, R. L. (2015). The effects of age on resting state functional connectivity of the basal ganglia from young to middle adulthood. *Neuroimage*, 107, 311–322.

Papenberg, G., Lindenberger, U. and Bäckman, L. (2015). Aging-related magnification of genetic effects on cognitive and brain integrity. *Trends in Cognitive Sciences*, 19, 506–514.

Petersen, S. E. and Posner, M. I. (2012). The attention system of the human brain: 20 years after. *Annual Reviews Neuroscience*, 35, 73.

Prince, M., Bryce, R., Albanese, E., Wimo, A., Ribeiro, W. and Ferri, C. P. (2013). The global prevalence of dementia: a systematic review and metaanalysis. *Alzheimer's & Dementia*, 9, 63–75.

Salvador, R., Suckling, J., Coleman, M. R., Pickard, J. D., Menon, D. and Bullmore, E. D. (2005). Neurophysiological architecture of functional magnetic resonance images of human brain. *Cerebral Cortex*, 15, 1332–1342.

Saunders, A. M. *et al.* (1993). Association of apolipoprotein E allele ϵ4 with late-onset familial and sporadic Alzheimer's disease. *Neurology*, 43, 1467–1467.

Sheline, Y. I. and Raichle, M. E. (2013). Resting state functional connectivity in preclinical Alzheimer's disease. *Biological Psychiatry*, 74, 340–347.

Sluimer, J. D. *et al.* (2008). Whole-brain atrophy rate and cognitive decline: longitudinal MR study of memory clinic patients 1. *Radiology*, 248, 590–598.

Song, X. W. *et al.* (2011). REST: a toolkit for resting-state functional magnetic resonance imaging data processing. *PloS One*, 6, e25031.

Sperling, R. A. *et al.* (2009). Amyloid deposition is associated with impaired default network function in older persons without dementia. *Neuron*, 63, 178–188.

Szczepanski, S. M. and Knight, R. T. (2014). Insights into human behavior from lesions to the prefrontal cortex. *Neuron*, 83, 1002–1018.

Tondelli, M., Wilcock, G. K., Nichelli, P., De Jager, C. A., Jenkinson, M. and Zamboni, G. (2012). Structural MRI changes detectable up to ten years before clinical Alzheimer's disease. *Neurobiology of Aging*, 33, 825–e25.

Vemuri, P. *et al.* (2010). Effect of apolipoprotein E on biomarkers of amyloid load and neuronal pathology in Alzheimer disease. *Annals of Neurology*, 67, 308–316.

Vergun, S. *et al.* (2013). Characterizing functional connectivity differences in aging adults using machine

learning on resting state fMRI data. *Frontiers in Computational Neuroscience*, 7, 38.

Wang, J., Wang, X., He, Y., Yu, X., Wang, H. and He, Y. (2015). Apolipoprotein E $\varepsilon 4$ modulates functional brain connectome in Alzheimer's disease. *Human Brain Mapping*, 36, 1828–1846.

Watanabe, T. *et al.* (2013). A pairwise maximum entropy model accurately describes resting-state human brain networks. *Nature Communications*, 4, 1370.

Wikenheiser, A. M. and Redish, A. D. (2012). Hippocampal sequences link past, present, and future. *Trends in Cognitive Sciences*, 16, 361–362.

Wu, X. *et al.* (2016). A triple network connectivity study of large-scale brain systems in cognitively normal APOE 4 carriers. *Frontiers in Aging Neuroscience*, 8, 231.

Xia, M., Wang, J. and He, Y. (2013). BrainNet viewer: the visualization tool a network for human brain connectomics pIoS one, 8.7, e68910.